Conducting Polymers

DOI: 10.1002/anie.200903596

Cathodic Deposition of Polypyrrole Enabling the One-Step Assembly of Metal–Polymer Hybrid Electrodes**

*Yongju Jung, Nikhilendra Singh, and Kyoung-Shin Choi**

Conducting polymers combining the advantages of organic polymers and the electronic properties of semiconductors are attractive materials for use in energy conversion/storage, optoelectronics, coatings, and sensing applications.[1–7] The polymerization process of conducting polymers initiates with chemical or electrochemical oxidation of monomers to radicals, which is followed by radical coupling and chain propagation.[2] Chemical oxidation involves the use of oxidizing agents, such as $FeCl_3$, while electrochemical oxidation is achieved by applying an anodic bias to a conducting substrate immersed in a monomer solution (anodic electropolymerization).[2,3] The electropolymerization method has been predominantly used to prepare film- or electrode-type conducting polymers, as it allows for polymerization confined to the working electrode with a facile control over film thickness and morphology.[3]

Conducting polymers have also been utilized as a matrix to embed or disperse metal particles (e.g., Cu, Au, Ag, Ni, Ru, Ir, Pt, Co, Pd, Fe) to form metal–polymer hybrid electrodes for use in sensors and electrocatalysts.[8–13] Typically, these hybrid electrodes are prepared by a two-step electrodeposition process: electropolymerization followed by metal deposition. This two-step process not only makes the synthesis cumbersome and expensive but also limits the types and qualities of the metal–polymer composite architectures that can be assembled. However, no synthesis strategy that enables one-step synthesis of metal–conducting polymer hybrid films has been made available to date. This is because electropolymerization and metal deposition require an oxidation and a reduction reaction at the working electrode, respectively, with a significantly different range of potentials.

Herein, we report an electrochemical method that allows cathodic deposition of polypyrrole (ppy) for the first time. The cathodic deposition method creates many new possibilities for assembling conducting-polymer and conducting-polymer-based hybrid electrodes that cannot be achieved by conventional anodic polymerization. First, conducting-polymer films or coatings can be deposited on substrates that are not stable under anodic deposition conditions. Second, the nucleation and growth processes of conducting polymers during cathodic deposition are different from those of anodic deposition, which results in new micro- and nanoscale polymer morphologies. Third, one-step electrodeposition of metal–conducting polymer hybrid electrodes becomes possible because both the polymerization and metal reduction reactions can occur under the same cathodic conditions. In this study, we demonstrate the use of cathodic polymerization for the production of high-surface-area ppy electrodes and the one-step synthesis of tin–ppy composite electrodes. The resulting tin–ppy electrodes were characterized for use as anodes in Li-ion batteries.

The cathodic deposition of conducting polymers was achieved by coupling two redox reactions. The first reaction is electrochemical generation of an oxidizing agent, the nitrosyl ion (NO^+). The production of NO^+ ions involves reduction of nitrate ions (NO_3^-) to nitrous acid (HNO_2) [Eq. (1)].[14,15] HNO_2 is amphoteric, and can generate various species in solution depending on the pH. Under mildly acidic conditions, HNO_2 is the major species but it dissociates into NO_2^- and H^+ as the pH increases ($pK_a = 3.3$).[16] In strongly acidic conditions, HNO_2 reacts with H^+ ions and generates the NO^+ ion [Eq. (2), pK_a of $H_2NO_2^+ = -7$], which is a strong oxidizing agent.[16–18]

$$NO_3^- + 3\,H^+ + 2\,e^- \leftrightarrow HNO_2 + H_2O \quad (1)$$

$$HNO_2 + H^+ \leftrightarrow H_2NO_2^+ \leftrightarrow NO^+ + H_2O \quad (2)$$

The second reaction is chemical oxidation of pyrrole by NO^+ ions, which initiates the polymerization process. Since the oxidizing agents are generated in situ only at the working electrode, polymerization occurs predominantly on the working electrode, which results in deposition of electrode-type or film-type conducting polymers at the cathode. Spectroscopic detection of electrochemically generated NO^+ ions and a study of pH-dependent NO^+ formation can be found in the Supporting Information (Figure S1). We believe that this is the first example of utilizing electrochemically generated NO^+ ions for cathodic deposition of a material that is typically obtained by anodic deposition.

The typical deposition conditions include the use of an aqueous solution containing 0.4 M HNO_3, 0.5 M $NaNO_3$, and 0.2 M pyrrole (the pH of the freshly made solution was 0.4) as a plating solution. The working electrode was copper foil and the counter electrode was 1000 Å of platinum deposited on 200 Å of titanium on a glass slide by sputter coating. Electrodeposition was carried out at $E = -0.65$ V versus an

[*] Dr. Y. Jung,[+] N. Singh,[+] Prof. K.-S. Choi
Department of Chemistry, Purdue University
West Lafayette, IN 47907 (USA)
Fax: (+1) 765-494-0239
E-mail: kchoi1@purdue.edu

[+] These authors contributed equally to this work.

[**] This work was supported by the Basic Energy Sciences Program of the US Department of Energy (DE-FG02-05ER15752) and made use of the Life Science Microscopy Facility at Purdue University. We thank Anna Kempa-Steczko for ICP–AES analysis.

Supporting information for this article is available on the WWW under http://dx.doi.org/10.1002/anie.200903596.

Ag/AgCl/4 M KCl reference electrode at room temperature. Efficient deposition of ppy films was possible only when the pH was lower than 1.5, because an appreciable amount of NO^+ species can be generated by electrochemical reduction of NO_3^- only in a strongly acidic environment.

Scanning electron microscopy (SEM) shows that the resulting ppy film contains spherical particles with diameters ranging from 50 to 200 nm creating a three-dimensional porous network, which can be highly beneficial for applications that require conducting-polymer electrodes with high surface areas (Figure 1 a). This morphology is unique in that

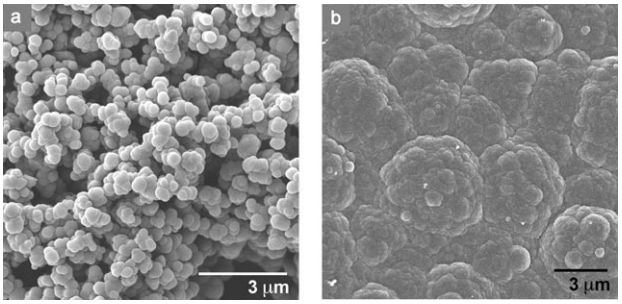

Figure 1. SEM images of ppy films deposited under a) cathodic ($E = -0.65$ V) and b) anodic conditions ($E = +0.80$ V) using an aqueous solution containing 0.4 M HNO_3, 0.5 M $NaNO_3$, and 0.2 M pyrrole (pH 0.4).

anodically prepared ppy films typically possess two-dimensional planar surface morphologies. An SEM image of a ppy film deposited anodically ($E = +0.80$ V vs. Ag/AgCl) using the same plating solution is shown in Figure 1 b for comparison. (A platinum working electrode was used in this case, as copper foil immediately oxidizes upon application of an anodic potential.) This film displays similar spherical features on the surface, but its surface is essentially two dimensional in nature and lacks mesoporosity.

The new cathodic polymerization method described above opens up a new possibility for preparing metal–conducting polymer hybrid electrodes through one-step deposition, because a broad range of metals can be cathodically deposited at the bias used to generate NO^+. During such a co-deposition process, new composite architectures can be generated because metal deposition and polymer deposition influence each other, thus altering their nucleation and growth patterns. In addition, co-deposition will increase the uniformity and degree of metal dispersion within the conducting-polymer matrix compared to a two-step deposition (anodic polymerization followed by metal deposition).

To demonstrate the effectiveness of this one-step synthesis, we assembled tin–ppy hybrid electrodes, which can be used as an anode material for Li-ion batteries.[19,20] The tin–ppy hybrid films were prepared by simply adding 0.1 M $SnCl_2$ to the plating solution used to deposit ppy films. Cathodic deposition was carried out at the identical potential used to deposit ppy films with the bath temperature increased to 45 °C to help dissolution of $SnCl_2$. The X-ray diffraction study of the resulting hybrid film showed the presence of a crystalline Sn phase as the only inorganic phase present in this film (Supporting Information, Figure S2).

SEM images of tin–ppy hybrid electrodes show that the hybrid film maintained the original ppy framework composed of ppy nanospheres creating a porous network (Figure 2 a).

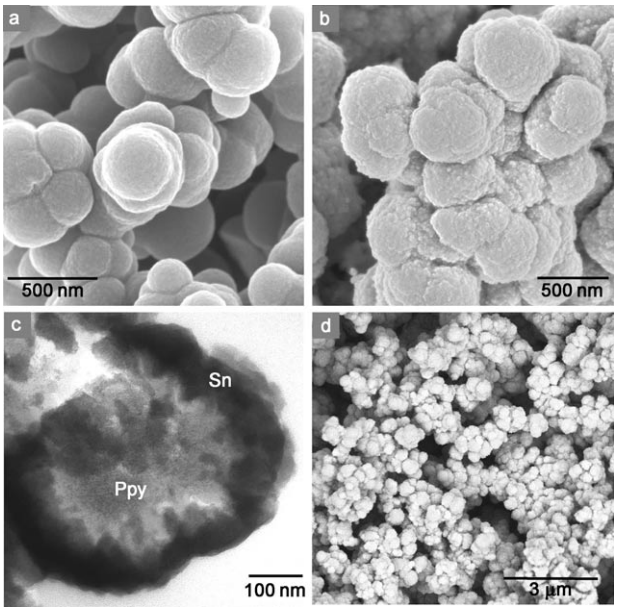

Figure 2. SEM images of a) pure ppy spheres and b) tin–ppy hybrid spheres. c) TEM image of a cross-sectioned tin–ppy hybrid sphere and d) BSE image of a tin–ppy hybrid electrode.

However, the surface of the ppy spheres became noticeably rough because of the presence of tin nanoparticles (Figure 2 b). A transmission electron microscopy (TEM) image of a cross-sectioned tin–ppy sphere shows that Sn particles are evenly coated on the surface of the ppy spheres (Figure 2 c). Analysis of multiple cross-sectional TEM images suggests that the thickness of the tin coating layer on the ppy spheres ranges from 25 to 100 nm. The uniformity of tin deposition on the ppy spheres could also be confirmed by taking a back-scattered electron (BSE) image (Figure 2 d). In the BSE image, tin particles with higher electron density should appear brighter than ppy spheres. The fact that all spheres displayed even contrast, instead of showing scattered and isolated brighter spots on the ppy spheres, indicates that the tin layers were formed uniformly on these spheres and no bare ppy surfaces were exposed at the surface.

Tin metal has been reported as an attractive anode material for high-energy-density Li-ion batteries because of its high theoretical specific capacity for lithium (993 mAh g^{-1}, corresponding to the formation of $Li_{4.4}Sn$).[19,20] However, its significant volume change upon insertion and extraction of lithium (up to 300 %) causes pulverization resulting in poor cycle performance, and has limited the use of tin anodes in commercial Li-ion batteries.[19,20] One of the most common approaches to overcoming this problem is to combine tin with an electrochemically inactive buffer matrix that can accommodate the volume change of tin during cycling.[21–24] Decreasing the size and increasing the degree of dispersion

of metallic tin in the matrix can be beneficial for improving the cycle properties, because the volume changes caused by smaller domains can be more easily accommodated by the matrix.[24] The use of tin nanoparticles can also be advantageous for increasing the rate capability, as it decreases the diffusion length of Li^+ ions to complete the alloying and dealloying processes.[24,25]

In this context, the tin–ppy hybrid morphologies shown in Figure 2 look promising for improving both cycle properties and rate capabilities. The ppy spheres can serve as an excellent buffer matrix that can elastically accommodate the volume expansion of nanoparticulate tin layers during cycling. In addition, the thin coating layers of tin on a highly porous ppy network will ensure facile Li-ion diffusion in and out of the anode, thus resulting in high rate capabilities. Another advantage of our hybrid electrode is the high weight content of tin in the anode (two-component system). Typically, the preparation of tin anodes involves mixing tin particles with a polymer binder and conducting additives (three-component system). In our case, however, the as-deposited tin–ppy electrode was used directly to assemble Li-ion batteries without any additional binding material or conducting additives, because tin particles were electrodeposited with an excellent adhesion to the ppy spheres and good electrical continuity between the particles within the tin layers. It is worth mentioning that the ppy does not serve as a conducting agent in the tin–ppy anode because ppy is not conductive in the potential range used for electrochemical evaluation of tin–ppy/Li cells ($0.0\,V \le E$ vs. $Li^+/Li \le 2.0\,V$).[26–28] As a result, the tin content in the hybrid electrode could be increased up to 95 wt%. The tin content in the hybrid electrodes used for electrochemical characterization discussed below was 88 wt% (determined by inductively coupled plasma–atomic emission spectroscopy).

The potential profiles of the tin–ppy hybrid electrodes for the initial two cycles (formation step) obtained at a rate of 0.2 C ($1\,C = 993\,mA\,g^{-1}$) are shown in Figure 3a (see the Supporting Information for experimental details). The coulombic efficiency for the first cycle (64%) was poor as a result of the high irreversible capacity observed during the first discharge process. This is typical behavior for systems containing nanostructured electrochemically active materials that create large electrode/electrolyte contact areas.[20] The high coulombic efficiency for the second cycle (94%) indicates that a stable solid-electrolyte interphase (SEI) was formed during the first cycle. The potential profiles of a pure tin electrode, which was electrochemically deposited using a sulfate bath and contained the same amount of tin as the hybrid electrode,[29,30] are shown in the Supporting Information (Figures S3 and S4) for comparison. Unlike the tin–ppy hybrid electrode, the pure tin electrode showed a drastic capacity decrease during the second discharge process.

The cycle performance and coulombic efficiency of the tin–ppy hybrid electrode up to 50 additional cycles after the formation step is shown in Figure 3b. A rate of 1 C was used for both charging and discharging processes. The initial capacity of the hybrid electrode, $942\,mAh\,g^{-1}$ of Sn, corresponds to $829\,mAh\,g^{-1}$ of composite (88 wt% of tin). This value is approximately 2.5 times larger than that of commercialized graphite anodes (ca. $330\,mAh\,g^{-1}$ of composite),[19] which suggests that with proper optimization the tin–ppy hybrid electrode may be used as anode material for future high-energy-density Li-ion batteries. After 50 cycles, the tin–ppy hybrid electrode showed a capacity retention of 47%. This is a remarkably enhanced performance compared to pure tin electrodes with a comparable thickness (ca. 10 μm), which typically show a severe capacity fading within a few cycles.[31] This finding suggests that the composite structure, in which ppy nanospheres provided a high-surface-area substrate to deposit tin as thin coating layers, efficiently suppressed pulverization and enhanced the cycling property of tin. Since the one-step production of tin–ppy electrodes did not require any more time or effort than electrodeposition of pure tin electrodes, the cathodic polymerization method

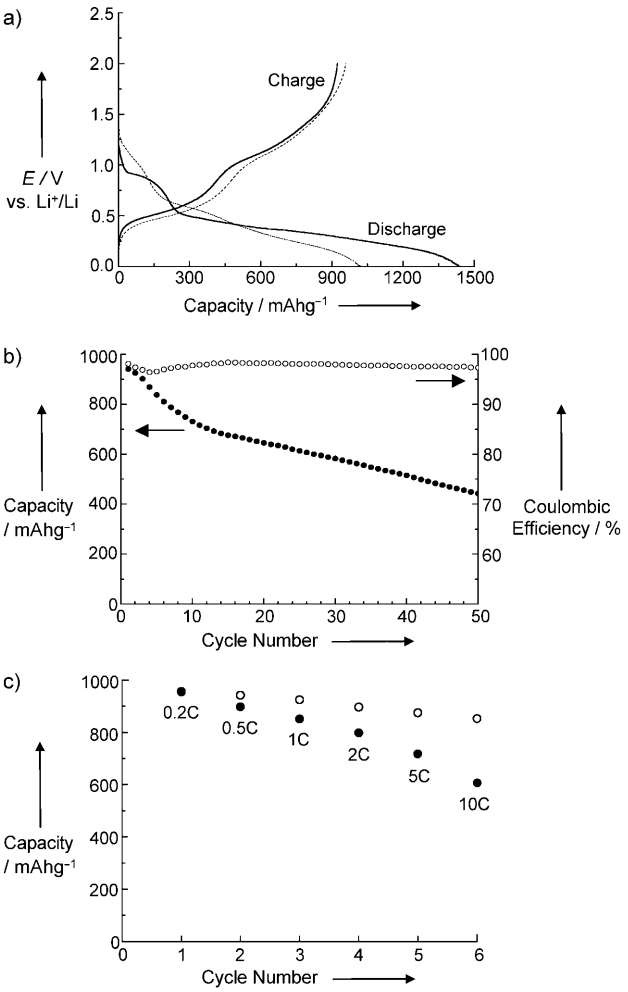

Figure 3. a) First (——) and second (•••••) charge/discharge curves of the as-prepared tin–ppy hybrid. b) Cycle properties of the tin–ppy hybrid electrode at a 1 C rate achieved after the formation step (charge capacity (●) and coulombic efficiency (○)). c) Rate capability of the tin–ppy hybrid electrode (●) achieved at various C rates after the formation step. The C rates for charging were changed sequentially through the cycles (0.2→0.5→1→2→5→10 C) whereas the discharge rate was fixed at 0.2 C. Data obtained at a fixed discharge/charge rate of 0.2 C through all cycles are also shown for comparison (○).

offered one of the most efficient and economic routes to enhance the performance of the tin anode.

The rate capabilities of the tin–ppy hybrid electrodes with varying C rates are shown in Figure 3c. Data obtained with a fixed discharge/charge rate of 0.2 C through all cycles are also shown for comparison. These data indicate that when the C rate was increased from 0.2 to 5 C, only an 18% reduction of the charge capacity was observed (from 875 to 718 $mAh\,g^{-1}$), which suggests the possibility of using tin–ppy hybrid electrodes as high-power-density as well as high-energy-density anodes. This outstanding rate capability is a result of the significant reduction of the diffusion length of Li ions required for complete utilization of tin in the hybrid structure. The results shown in Figure 3 were obtained from as-deposited tin–ppy electrodes. Therefore, further enhancements in capacity retention and rate capability are expected with proper optimization efforts (e.g., composition and morphology tuning in the hybrid electrodes, addition of a protective coating on the tin layer).[25,32,33]

In summary, we have developed a new synthesis strategy that enables cathodic deposition of conducting polymers by utilizing cathodically generated oxidizing agents for oxidative chemical polymerization of conducting polymers. This method enabled not only the synthesis of conducting polymers with new nanoscale morphologies but also the one-step synthesis of metal–conducting polymer hybrid electrodes. Because of the ability of cathodic polymerization to combine a variety of conducting polymers and metals with new composite architectures in a simple and cost-effective manner, the method described in this study will significantly broaden our ability to fabricate conducting-polymer and conducting-polymer-based composite electrodes for use in various applications.

Received: July 2, 2009
Published online: September 28, 2009

Keywords: cathodic deposition · conducting materials · hybrid electrodes · polymers · tin

[1] H. Shirakawa, E. J. Louis, A. G. MacDiarmid, C. K. Chiang, A. J. Heeger, *J. Chem. Soc. Chem. Commun.* **1977**, 578 – 580.
[2] J. Jang, *Adv. Polym. Sci.* **2006**, *199*, 189 – 259.
[3] S. Sadki, P. Schottland, N. Brodie, G. Sabouraud, *Chem. Soc. Rev.* **2000**, *29*, 283 – 293.
[4] E. Bundgaard, F. C. Krebs, *Sol. Energy Mater. Sol. Cells* **2007**, *91*, 954 – 985.
[5] P. Novák, K. Müller, K. S. V. Santhanam, O. Haas, *Chem. Rev.* **1997**, *97*, 207 – 281.
[6] B. Adhikari, S. Majumdar, *Prog. Polym. Sci.* **2004**, *29*, 699 – 766.
[7] G. Gustafsson, Y. Cao, G. M. Treacy, F. Klavetter, N. Colaneri, A. J. Heeger, *Nature* **1992**, *357*, 477 – 479.
[8] J. Y. Lee, T.-C. Tan, *J. Electrochem. Soc.* **1990**, *137*, 1402 – 1408.
[9] D. K. Sarkar, X. J. Zhou, A. Tannous, K. T. Leung, *J. Phys. Chem. B* **2003**, *107*, 2879 – 2881.
[10] M. Trueba, S. P. Trasatti, S. Trasatti, *Mater. Chem. Phys.* **2006**, *98*, 165 – 171.
[11] E. Navarro-Flores, S. Omanovic, *J. Mol. Catal. A* **2005**, *242*, 182 – 194.
[12] S. A. Meenach, J. Burdick, A. Kunwan, J. Wang, *Small* **2007**, *3*, 239 – 243.
[13] J. Li, X. Lin, *Sens. Actuators B* **2007**, *124*, 486 – 493.
[14] O. W. J. S. Rutten, A. Van Sandwijk, G. Van Weert, *J. Appl. Electrochem.* **1999**, *29*, 87 – 92.
[15] M. Pourbaix, *Atlas of Electrochemical Equilibria in Aqueous Solutions*, 2nd ed., National Association of Corrosion Engineers, Houston, **1974**, p. 384.
[16] A. F. Holleman, E. Wiberg in *Inorganic Chemistry* (Ed.: N. Wiberg), Academic Press, San Diego, **2001**, pp. 661 – 667.
[17] D. L. H. Williams, *Nitrosation*, Cambridge University Press, Cambridge, **1988**.
[18] G. A. Olah, R. Malhotra, S. C. Narang, *Nitration: Methods and Mechanisms*, VCH, New York, **1989**.
[19] J.-M. Tarascon, M. Armand, *Nature* **2001**, *414*, 359 – 367.
[20] A. S. Aricò, P. Bruce, B. Scrosati, J.-M. Tarascon, W. Van Schalkwijk, *Nat. Mater.* **2005**, *4*, 366 – 377.
[21] J. Fan, T. Wang, C. Yu, B. Tu, Z. Jiang, D. Zhao, *Adv. Mater.* **2004**, *16*, 1432 – 1436.
[22] P. G. Bruce, B. Scrosati, J.-M. Tarascon, *Angew. Chem.* **2008**, *120*, 2972 – 2989; *Angew. Chem. Int. Ed.* **2008**, *47*, 2930 – 2946.
[23] M. Winter, J. O. Besenhard, *Electrochim. Acta* **1999**, *45*, 31 – 50.
[24] J. Hassoun, S. Panero, P. Simon, P. L. Taberna, B. Scrosati, *Adv. Mater.* **2007**, *19*, 1632 – 1635.
[25] H. Lee, J. Cho, *Nano Lett.* **2007**, *7*, 2638 – 2641.
[26] T. V. Vernitskaya, O. N. Efimov, *Russ. Chem. Rev.* **1997**, *66*, 443 – 457.
[27] I. Rodríguez, B. R. Scharifker, J. Mostany, *J. Electroanal. Chem.* **2000**, *491*, 117 – 125.
[28] M. J. L. Santos, A. G. Brolo, E. M. Girotto, *Electrochim. Acta* **2007**, *52*, 6141 – 6145.
[29] S. D. Beattie, T. Hatchard, A. Bonakdarpour, K. C. Hewitt, J. R. Dahn, *J. Electrochem. Soc.* **2003**, *150*, A701 – A705.
[30] M. Inaba, T. Uno, A. Tasaka, *J. Power Sources* **2005**, *146*, 473 – 477.
[31] J. W. Park, J. Y. Eom, H. S. Kwon, *Electrochem. Commun.* **2009**, *11*, 596 – 598.
[32] M. Noh, Y. Kwon, H. Lee, J. Cho, Y. Kim, M. G. Kim, *Chem. Mater.* **2005**, *17*, 1926 – 1929.
[33] Y. Kwon, H. Kim, S.-G. Doo, J. Cho, *Chem. Mater.* **2007**, *19*, 982 – 986.

